Published in final edited form as:

Biochemistry. 2019 February 19; 58(7): 951–964. doi:10.1021/acs.biochem.8b01253.

A new class of phosphoribosyltransferase involved in cobamide biosynthesis is found in methanogenic archaea and cyanobacteria

Victoria L. Jeter[1], **Theodoric A. Mattes**[1,§], **Nathaniel R. Beattie**[2], and **Jorge C. Escalante-Semerena**[1,*]

[1]Department of Microbiology, University of Georgia, Athens, GA 30602

[2]Department of Biochemistry & Molecular Biology University of Georgia, Athens, GA 30602

Abstract

Cobamides (Cbas) are coenzymes used by cells from all domains of life, but made *de novo* only by some bacteria and archaea. The last steps of the cobamide biosynthetic pathway activate the corrin ring and the lower ligand base, condense the activated intermediates, and dephosphorylate the product prior to the release of the biologically active coenzyme. In bacteria, a phosphoribosyltransferase (PRTase) enyzme activates the base into its α-mononucleotide. The enzyme from *Salmonella enterica* (*Se*CobT) has been extensively biochemically and structurally characterized. The crystal structure of the putative PRTase from the archaeum *Methanocaldococcus jannaschii* (*Mj*CobT) is known but its function has not been validated. Here we report the *in vivo* and *in vitro* characterization of *Mj*CobT. *In vivo*, *in vitro*, and phylogenetic data reported here show that *Mj*CobT belongs to a new class of NaMN-dependent PRTase. We also show that the *Synechococcus* sp. WH7803 CobT protein has PRTase activity *in vivo*. Lastly, results of isothermal titration calorimetry and analytical ultracentrifugation analysis show that the biologically active form of *Mj*CobT is a dimer, not a trimer, as suggested by its crystal structure.

Graphical Abstract

*Corresponding author: Department of Microbiology, University of Georgia, 212C Biological Sciences Building, 120 Cedar Street, Athens, GA 30602, USA; Tel: +1 (706) 542-2651, Fax: (+1 (706) 542-2815, jcescala@uga.edu, www.escalab.com.

§ Present address: Department of Genetics, University of Georgia, Athens, GA 30602

UniProtKB Protein IDs

*Mj*CobT (UniProtKB Q58993)

*Se*CobT (UniProtKB Q05603)

*Syn*CobT (UniProtKB A5GMZ1)

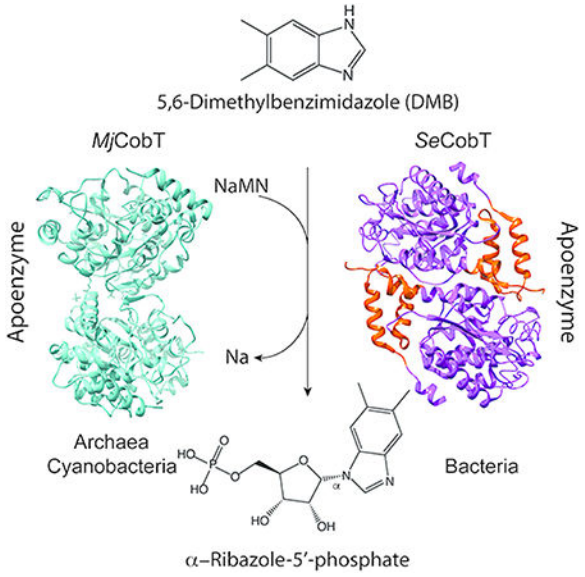

The activation of the lower ligand base of cobalamin is catalyzed by a new class of phosphoribosyltransferase found in archaea and cyanobacteria. The enzyme from the methanogenic archaeum *Methanocaldococcus jannaschii* (*MjCobT*) uses the same substrates but it is structurally different than the best studied bacterial enzyme from *Salmonella enterica* (*Se*CobT).

Keywords

CobT phosphoribosyltransferase; cyanobacteria; B_{12} biosynthesis; cobamides; *Methanocaldococcus jannaschii*; archaeal PRTase

INTRODUCTION

Cobamides (Cba) are cobalt-containing cyclic tetrapyrroles used by cells from all domains of life but are produced *de novo* only by some bacteria and archaea [reviewed in[1]]. Cbas are involved in enzymatic carbon skeleton rearrangements, methyl-group transfers, reductive dehalogenation, and elimination reactions[2–6]. Additionally, cobamide-dependence is common amongst radical SAM enzymes[7]. Recent work has identified a role for Cbas in gene regulation as photoreceptors (reviewed in[8]).

Structurally, Cbas are characterized by a central cobalt ion equatorially coordinated by the nitrogens of the pyrrole rings. Unlike other cyclic tetrapyrroles (*e.g.*, heme, factor F_{430}, bacteriochlorophylls), most Cbas contain an upper and a lower ligand. The coenzymic form of the Cba known as cobalamin (Cbl) has a 5’-deoxyadenosyl (Ado) group as its upper ligand and 5,6-dimethylbenzimidazole (DMB) as the lower ligand (Fig. 1A). In addition to DMB, other purines and benzimidazole homologues can serve as the lower ligand and form a coordination bond with the central cobalt ion[9] (Fig. 1B,C). Some organisms (*e.g.*, *Sporomusa ovata*) can also incorporate phenolics as bases into Cbas (Fig. 1D), but such bases cannot form coordination bonds with the cobalt ion of the ring.

Vitamin B_{12} (cyanocobalamin, CNCbl) is a Cba whose upper ligand is a cyano (CN) group, and its lower ligand is DMB. As shown in figure 1, the diversity of bases found in Cbas is broad[4, 9]. For example, *Salmonella enterica* produces three Cbas with varying nucleotide bases: one with DMB (a.k.a. cobalamin, Cbl), one with adenine (a.k.a. pseudocobalamin, psCbl), and one with 2-methyladenine (a.k.a. Factor A)[10–12].

Lower ligand bases require activation to an α-ribotide prior to their incorporation into the final product of the pathway. In *Salmonella enterica*, the CobT enzyme (EC 2.4.2.21), a nicotinate mononucleotide (NaMN):Base phosphoribosyltransferase (PRTase), activates the lower ligand base. The product of this reaction is the intermediate known as α-ribazole-5'-phosphate (α-RP) (Fig. 2)[13].

The last steps of AdoCba biosynthetic pathways activate the corrin ring and the lower ligand base, condense the activated intermediates into an AdoCba-phosphate (AdoCba-P), and, finally, removes the phosphate to yield the final product of the pathway (Fig. 3).

Previous *in vitro* studies of *Se*CobT showed that the enzyme has a broad range of substrate specificity and can activate purine and benzimidazole analogues (Fig. 1)[13, 14]. This lack of substrate specificity is shared by *S. enterica* CobT (*Se*CobT) homologues in other microorganisms[15]. At present, we know little about the function of archaeal *Se*CobT homologues. The crystal structure of the putative apo NaMN:Base PRTase from the methanogenic archaeum *Methanocaldococcus jannaschii* (ORF MJ_RS08515) has been reported, but evidence supporting the annotated activity has not been published.

Bioinformatics analyses of the MJ_RS08515 amino acid sequence compared with that of the *Se*CobT enzyme showed limited identity (18%) and similarity (32%) (Fig. 4). These enzymes also differed in their oligomeric state, with the archaeal enzyme forming trimers (PDB 3L0Z), according to the structure deposited into the Research Collaboratory for Structural Bioinformatics Protein Database (RCSB PDB) (unpublished work), while the bacterial enzyme forms dimers[13] (PDB 1L4B).

We note that previous studies by other investigators suggested that cyanobacteria solely produce psCbl. Additionally, these studies showed that 121 of the 123 cyanobacterial genomes searched lacked *cobT*[16, 17]. In contrast to these findings, our bioinformatics analysis identified CobT homologues in many cyanobacterial genomes. These homologues were similar in amino acid sequence composition to MJ_RS08515.

The work reported here shows that *M. jannaschii* CobT (*Mj*CobT) belongs to a new class of base-activating PRTase enzymes. We determined that *Mj*CobT represents a new class of base-activating PRTase enzymes based on both structural and taxonomic differences from the extensively characterized *Se*CobT. In this study we used *S. enterica* as a heterologous complementation system to show that *Mj*CobT has *bona fide* NaMN:DMB PRTase activity *in vivo*. Consistent with our *in vivo* results, *Mj*CobT exhibited robust enzymatic activity *in vitro* at pH 7. We found that under the conditions used to assay *Mj*CobT activity, the *Se*CobT enzyme also displayed strong activity. This finding was of interest, because in the past we had only measured strong *Se*CobT activity at pH 10. We identify potassium phosphate (KP_i) as the ingredient of the reaction mixture needed by *Se*CobT to be active at

pH 7. We also report that *MjCobT* has broad substrate specificity and high affinity for its NaMN substrate. Finally, our data support the idea that *Mj*CobT is biologically active as a dimer.

MATERIALS AND METHODS

Culture media and growth conditions.

All chemicals were reagent grade and were purchased from Sigma-Aldrich unless otherwise stated. Purchased chemicals were used without further purifications. All strains used in this study were grown at 37°C in no-carbon energy (NCE) minimal medium[18] supplemented with ribose (20 mM) as a carbon and energy source. Minimal medium was also supplemented with $MgSO_4$ (1 mM) and trace minerals[19]. When used, ampicillin, kanamycin, or chloramphenicol were added at 100 μg/mL, 50 μg/mL or 25 μg/mL, respectively. For all growth experiments, two μL of overnight cultures (12–16 h old) grown in nutrient broth (NB, Difco) was used to inoculate 198 μL of minimal medium with supplements (1% inoculum, v/v). Strains were grown in triplicate in 96-well microtiter plates for growth experiments. Growth was monitored using a computer-controlled BioTek plate reader (Model Eon). Optical density at 630 nm was measured every 30 min for a total time of 24 h; the microtiter dish was shaken between measurements. Data were analyzed using GraphPad Prism v6 software. Doubling times were calculated using the exponential growth equation included with the GraphPad Prism v6 software.

Strain constructions.

All strains used in in this study were derivatives of *Salmonella enterica enterica* sv Typhimurium (hereafter *S. enterica*) LT2 or *Escherichia coli* BL21. Strain genotypes are described in Table S1. Plasmids were introduced into *S. enterica* by electroporation[20] and into *E.coli* by heat-shock transformation[21]. Deletions in *S. enterica* were constructed and resolved with pCP20 as described elsewhere[22].

Plasmid constructions.

All primers used during the course of this work are described in Table S2. Restriction enzymes were purchased from Fermentas. BspQI restriction enzyme was purchased from New England BioLabs. *Synechococcus* sp. WH7803 cobT gene was codon optimized for expression in *E. coli* by GenScript (Fig. S1).

Plasmid pMjCobT1.

This plasmid was constructed using the polymerase incomplete primer extension (PIPE) method[23]. The *Methanocaldococcus jannaschii* wildtype allele of ORF MJ_RS08515 was amplified from *M. jannaschii* genomic DNA (a gift from W. B. Whitman, University of Georgia) using the primers Mj_1598_cobT_PIPE_f and Mj_1598_cobT_PIPE_r. Vector pBAD24[24] was amplified using primers pBAD24-PIPE-5’ and pBAD24-PIPE-3’. Amplified fragments were cut with DpnI (ThermoFisher) overnight at 37°C. Fragments were mixed in equal volumes and transformed in chemically competent *E. coli* DH5a[21]. The completed plasmid contained ORF MJ_RS08515 coding sequence inserted between KpnI and SalI sites of pBAD24. The plasmid was used for complementation analyses and generation of

cobamides in *S. enterica*. Plasmid pMjCobT1 is 5,601 bp long and encodes resistance to ampicillin.

Plasmid pMjCobT2.

This plasmid was also constructed using the PIPE method as described above using primers Mj_1598_TEV5_PIPE_f and Mj_1598_TEV5_PIPE_r to amplify ORF MJ_RS08515 and primers pTEV5-PIPE-5' and pTEV5-PIPE-3' to amplify the pTEV5 vector[25]. pMjCobT2 contained the wildtype MJ_RS08515 coding sequence inserted between NheI and XhoI sites of pTEV5. pMjCobT2 was used for protein overproduction. The plasmid is 6,381 bp long and encodes resistance to ampicillin. Transcription of MJ_RS08515 was induced by the addition of isopropyl-β-D-1-thiogalactopyranoside (IPTG), which triggered the synthesis of T7 polymerase, the enzyme responsible for the transcription of MJ_RS08515.

Plasmid pCOBT140.

The construction of this vector has been described[26]. The plasmid encodes *S. enterica cobT* $^{+}$, is ~5.6 kb long and encodes ampicillin resistance.

Plasmid pMjCobT3.

This plasmid encoded *Mj*CobT^{E315A} and was constructed using overlapping primers MjCobT_sdm_E315A_F and MjCobT_sdm_E315A_R with plasmid pMjCobT1 DNA as the template. Briefly, the primers indicated encoding E315A changes were used to amplify the ORF MJ_RS08515 on pMjCobT1. Amplified products were cut with DpnI (ThermoFisher) overnight at 37°C. The amplification product was then transformed in *E. coli* DH5a and its nucleotide sequence verified.

Plasmid pMjCobT4.

This plasmid encoded variant *Mj*CobT$^{E150A\ E315A}$ and was constructed using overlapping primers MjCobT_sdm_E150A_F and MjCobT_sdm_E150A_R with plasmid pMjCobT3 DNA as the template. Briefly, the primers indicated encoding E150A changes were used to amplify the ORF MJ_RS08515 with the E315A change on pMjCobT3. Amplified products were cut with DpnI (ThermoFisher) overnight at 37°C. The amplification product was then transformed in *E. coli* DH5a and its nucleotide sequence verified.

Plasmid pMjCobT5.

This plasmid encoded *Mj*CobT^{E150A} and was constructed using overlapping primers MjCobT_sdm_E150A_F and MjCobT_sdm_E150A_R with plasmid pMjCobT1 DNA as the template. Briefly, the primers encoding E150A changes were used to amplify the ORF MJ_RS08515 on pMjCobT1. Amplified products were cut with DpnI (ThermoFisher) overnight at 37°C. The amplification product was then transformed in *E. coli* DH5a and its nucleotide sequence verified.

Plasmid pSynCobT2.

This plasmid was constructed using the BspQI high-efficiency cloning method outlined elsewhere[27] using primers SynCobT pCV1 F and SynCobT pCV1 R to amplify the codon

optimized *Synechococcus* sp. WH7803 CobT (SYNWH7803_RS09275). The completed plasmid contained codon optimized SYNWH7803_RS09275 coding sequence inserted between the pair of BspQI sites of pCV1. The plasmid was used for complementation analyses in *S. enterica*. Plasmid pSynCobT2 is 5,724 bp long and encodes resistance to ampicillin.

Cobamide extraction and high-performance liquid chromatography (HPLC) analysis.

Overnight culture of strain JE18114 (Δ*metE* Δ*cobT* Δ*cobB* / pMjCobT1) and strain JE18115 (Δ*metE* Δ*cobT* Δ*cobB* / pCOBT140) grown in nutrient broth (NB) supplemented with ampicillin (100 μg/mL), kanamycin (50 μg/mL), and chloramphenicol (25 μg/mL) was used to inoculate NCE minimal medium supplemented with ribose (20 mM) as a carbon and energy source. Minimal medium also contained trace minerals, magnesium sulfate (1 mM), ampicillin (100 μg/mL) arabinose (500 μM), and dicyanocobinamide [$(CN)_2$Cbi] (300 nM). Where indicated, DMB, adenine, 5-methoxybenzimidazole (5-MeO-Bza), or 5-hydroxybenzimidazole (5-HO-Bza) was provided at a final concentration of 200 μM. Cultures (250 mL) were grown for >20 h at 37°C in an Innova 44R gyratory incubator (New Brunswick Scientific) shaking at 180 rpm. Cells were harvested by centrifugation at 4°C for 15 min at 6,000 × *g* using an Avanti J20-XPI refrigerated centrifuge (Beckman) equipped with JLA-8.1000 rotor. Pelleted cells were re-suspended in ammonium acetate buffer (100 mM, pH 4.5) containing KCN (10 mM), and stored at −20 °C. Cobamides were extracted using methods described elsewhere[28, 29]. Cell suspensions were thawed on ice and subsequently incubated at 70°C with shaking at 180 rpm in an Innova 44R gyratory incubator (New Brunswick Scientific) for 2 h. After incubation, cell suspensions were centrifuged in an Avanti J-251 equipped with a JA 25.25 rotor (Beckman) at 43,000 × *g* for 40 min at 4°C. Clarified cell-free extract was filtered through a syringe filter unit (0.45 μm) and mixed with Amberlite XAD4 resin (Rohm-Haas). Cell-free extract and resin mixtures were incubated at 37°C with shaking at 180 rpm in an Innova 43 gyratory incubator (New Brunswick Scientific) for 16 h. After allowing the resin to settle, free liquid was removed, taking care not to disturb the resin. Resin was washed thrice with four bed volumes of deionized water (Millipore) allowing the resin to settle for 20 min between washes. After the final wash, two bed volumes of methanol (100%) were added to the resin and the solution incubated 16 h at room temperature. After incubation, methanol was removed from the resin, collected in a microfuge tube and subjected to vacuum centrifugation in an Eppendorf Vacufuge Plus set at 60 °C until dry. Dried pellets were re-suspended in a 1:4 ratio of buffer B [KH_2PO_4 (100 mM), KCN (10 mM), pH 8 + 50% (v/v) acetonitrile] and buffer C [KH_2PO_4 (100 mM), KCN (10 mM), pH 6.5] in preparation for separation by HPLC. Cbas were resolved by RP-HPLC using a Shimadzu Prominence UFLC SPD-M30A equipped with a Phenomenex Syngergi 4μ hydro-RP80A 150 × 4.6 mm LC column as described[30, 31] with some modifications as outlined in[26]. Cbas were detected at 367 nm and 525 nm.

Mass spectrometry of corrinoids.

Corrinoids with retention times of 12, 13, and 16 min were collected, desalted using C18 SepPaks (Waters) and dried under vacuum centrifugation. The molecular mass of each corrinoid was determined by MALDI-TOF mass spectrometry at the PAMS facility of the University of Georgia.

Protein purification.

Wild-type *Mj*CobT protein was overproduced from plasmid pMjCobT2 in strain JE6663 (*E. coli* C41) in 2-L cultures of Terrific Broth[32]. Protein synthesis was induced by the addition of IPTG at a final concentration of 500 μM in mid-log phase cultures (OD_{600} ~0.6) growing at 37°C with shaking at 180 rpm in an Innova44 (New Brunswick Scientific) gyratory incubator. After induction, cultures were grown for 17 h at 30°C with shaking at 180 rpm. Cultures were harvested by centrifugation at 4°C for 15 min at 6,000 × *g* in an Avanti J20-XPI refrigerated centrifuge equipped with JLA-8.1000 rotor. Pelleted cells were stored at −80°C until used. Frozen cells were thawed on ice and re-suspended in Tris-HCl buffer (25 mM, pH 7.5) containing NaCl (0.5 M) and imidazole (20 mM) at a rate of 20% cell weight to buffer volume. Lysozyme (1μg/mL) and DNaseI (25μg/mL) were added to the cell suspension and incubated on ice for 10 min. Cells were lysed by cell press in a cell disruptor (Constant Systems) set at 1.72e8 Pa. Phenylmethylsulfonyl fluoride (PMSF) was added to the cell lysate at a final concentration of 0.5 mM. The cell lysate was incubated for 30 min at 70°C to precipitate *E. coli* proteins. Cell debris and precipitated proteins were removed by centrifugation at room temperature for 30 min at 40,000 × *g* in an Avanti J-251 centrifuge (Beckman/Coulter) equipped with a JA 25.25 rotor. Clarified extract was filtered using a 0.45-μm syringe filter unit and applied to a 4-mL HisPur nickel-nitrilotriacetic acid (Ni-NTA) affinity column (ThermoFisher Scientific). The column was washed with 10 column volumes of Tris-HCl buffer (25 mM, pH 7.5) containing NaCl ((0.5 M) and imidazole (20 mM) and six column volumes of Tris-HC buffer (25 mM, pH 7.5) containing NaCl (0.5 M)) and imidazole (40 mM). H_6-*Mj*CobT was eluted with six column volumes of Tris-HCl buffer (25 mM, pH 7.5) containing NaCl (0.5 M) and imidazole (0.5 M). Fractions were collected throughout the wash and elution steps and H_6-*Mj*CobT purification was monitored by SDS-PAGE gel compared to Precision Plus Protein Standards (BioRad). Fractions containing H_6-*Mj*CobT were pooled and dialyzed against Tris-HCl buffer (25 mM, pH 7.5) containing NaCl (0.5 M) to remove imidazole. N-terminally tagged, recombinant tobacco etch virus protease (H_7-rTEV) was purified as described elsewhere[33] and mixed with H_6-*Mj*CobT at a ratio of 1:10 H_6-*Mj*CobT:H_7-rTEV. The mixture was incubated at 34°C for 3 h to remove the H_6 tag on *Mj*CobT. Cleaved *Mj*CobT was purified away from the tag and H_7-rTEV using the Ni-NTA affinity purification method outlined above and tag-less protein was dialyzed against Tris-HCl buffer (25 mM, pH 7.5) in steps with decreasing concentrations of NaCl down to 150 mM. Purified *Mj*CobT was flash frozen in liquid nitrogen and stored at −80°C until used. Protein concentration was measured using a NanoDrop 1000 spectrophotometer (Thermo Scientific) using the molecular mass of 37600 Da and ε_{280} of 20400 M^{-1} cm^{-1} as determined by ProtParam[33].

Analytical ultracentrifugation.

*Mj*CobT was dialyzed against 50 mM Na/K phosphate (pH 7.5) and 100 mM NaCl and diluted to a final concentration of 1 mg/ml. Quantification was performed on an Agilent 8453 UV/vis and used an ε_{280} of 20400 M^{-1} cm^{-1} as determined by ProtParam[34]. The protein sample was loaded with the dialysis buffer to a final concentration of 1 mg/ml before being loaded into cells with 12 mm double-sector Epon centerpieces. The loaded cells were allowed to equilibrate in the rotor for 1 h at 20 °C. Sedimentation velocity data were collected at 50,000 rpm at 20 °C in an Optima XLA analytical ultracentrifuge. Data were

recorded at 280 nm in radial step sizes of 0.003 cm. SEDNTERP[35] was used to calculate the partial specific volume of *Mj*CobT (0.756018 mL/g) as well as[363535] the density (1.0093 g/mL) and viscosity coefficient (0.010291) of the buffer. SEDFIT[37] was used to analyze the raw sedimentation data. Data were modeled as a continuous sedimentation coefficient distribution [c(s)], and were fit using the baseline, meniscus, frictional coefficient, and systematic time-invariant and radial-invariant noise. Fit data for the experiment had a root mean square deviations of (r.m.s.d) < 0.004 AU. The theoretical sedimentation coefficient (s) values were calculated from the atomic coordinates of *Mj*CobT(PDB ID 3L0Z) using HYDROPRO20[38].

In vitro NaMN:DMB phosphoribosyltransferase assay.

NaMN:DMB PRTase activity was assayed as described elsewhere with minor changes to the reaction conditions detailed in each of the following sections[13]. Asterisks shown represent the following *p*-values: * denotes a *p*-value <0.05, ** denotes a *p*-value <0.01, *** denotes a *p*-value <0.001.

Specific activity measurements.

To determine the specific activity of *Mj*CobT, the protein was diluted in potassium phosphate buffer (0.25 M, pH 8.0). Reaction mixtures contained phosphate buffer (0.25 M, pH 8.0), DMB (1.5 nmol), [2-^{14}C]-DMB (0.5 nmol) and *Mj*CobT (190 ng) in a final volume of 20 μL. NaMN was provided in the following amounts: 20, 15, 10, and 5 nmoles. Reactions mixtures were incubated at 37°C. Samples were removed after 0, 3, 5, 10, and 15 min incubations and immediately spotted (5 μL) onto a silica gel thin-layer chromatography (TLC) plate (Whatman PE SIL G/UV). TLCs were developed for 1.5 h in a TLC chamber pre-equilibrated with a 3:2 (v/v) chloroform:methanol mobile phase. After drying in a fume hood, plates were exposed to a phosphor screen for 18 h. Distribution of radioactivity on TLC plates was visualized using a Typhoon Trio+ Variable Mode Imager (GE Life Sciences) with ImageQuant v5.2. Pixel density of TLC plates was analyzed using 1D gel analysis in TotalLab TL100 (Nonlinear Dynamics) and the resulting data were analyzed using Prism v6 (GraphPad). Each reaction was performed in triplicate.

Effect of pH on *Mj*CobT activity.

Reactions were conducted as outlined above with NaMN (1 mM) and buffer (25 mM) at the following pHs: sodium malate, pH 5, sodium succinate, pH 5.5, 4- morpholineethansulfonic acid (MES) pH 6, Bis-Tris pH 6.5, imidazole pH 7, Tris-HCl, pH 7, Tris-HCl pH 8, potassium phosphate pH 8, Tris-HCl pH 9, 2-(cyclohexylamino)ethanesulfonic acid (CHES) pH 9, CHES pH 9.5, glycine pH 10, and glycine pH 10.5. Reaction mixtures were incubated for 15 min at 37°C.

Effect of ionic strength on *Mj*CobT activity.

Varying concentrations of salt tested as outlined above with NaMN (1 mM) and either potassium chloride or sodium chloride at the following concentrations: 0.1, 0.2, 0.3, 0.4 and 0.5 M. Reaction mixtures were incubated for 15 min at 37 °C.

Effect of temperature on *Mj*CobT activity.

*Mj*CobT activity as a function of incubation temperature was tested as outlined above with NaMN (1 mM). Reactions were incubated for 10 min at 40, 50, 70, or 80°C.

Effect of phosphate on *Mj*CobT activity.

*Mj*CobT activity as a function of phosphate concentration was measured as described above with NaMN (1 mM) and phosphate at either 0.025, 0.05, 0.075, 0.1, 0.2 or 0.4 M phosphate salts adjusted to pH 7.0. Reaction mixtures were incubated for 15 min at 80°C. Equivalent reactions were prepared with sodium salts of sulfate, vanadate, selenate, or molybate in lieu of potassium phosphate for comparison.

Determination of kinetic parameters.

Pseudo-first order kinetic data were obtained at a range of NaMN concentrations (0.075 to 1 mM) with a saturating concentration of DMB (100 μM). The data were fit to the Michaelis-Menten equation to determine the K_m and maximum velocity (V_{max}):

$$v = \frac{V_{max}[S]}{K_m + [S]}$$

The turnover constant (k_{cat}) was obtained with the following equation where E represents enzyme concentration:

$$k_{cat} = \frac{V_{max}}{E}$$

Catalytic efficiency was determined by the following: k_{cat}/K_m.

Isothermal titration calorimetry.

Binding assays of *Mj*CobT and NaMN substrate were performed using a Nano ITC isothermal titration calorimeter (TA instruments). *Mj*CobT was dialyzed against Tris-HCl buffer (25 mM, pH 7.5) containing NaCl (150 mM); NaMN was solubilized in the final protein dialysate. Samples were degassed for 20 min at 25°C before use. *Mj*CobT protein was present in the sample cell at 33 μM under constant stirring at 350 rpm, and NaMN was present in the injection syringe at 1 mM. Every 5 min, injections (2.4 μL) were made into the sample cell and heat released was recorded. Experiments were conducted at 25°C. Data were analyzed using NanoAnalyze software (TA instruments).

Phylogenetic analysis.

We searched for *Mj*CobT homologues using NCBI BLASTP with CobT query sequences from *M. jannaschii* (accession: WP_064496984.1), *S. enterica* (accession: NP_460961.1), *P. denitrificans* (accession: WP_015478315.1), and *B. megaterium* (accession: YP_003563500.1)[39]. Query sequences were used to search cyanobacteria (taxid: 1117), thaumarchaeota (taxid: 651137), methanogens class I (taxid: 2283794), and methanogens class II (taxid: 224756). Results with a minimum 85% query coverage and e-value cutoff of

$<10^{-40}$ were included in the supplementary tables. Results were screened using the NCBI conserved domain database (CDD) to confirm DMB-PRT_CobT superfamily (accession: cl11435, PSSM Id: 325029) placement[40]. The percent identity and percent positives are also provided. Results from "uncultured marine thaumarchaeotes" were omitted from the tables.

The phylogenetic tree (Fig. 14) was constructed using SeaView software[41]. CobT homologue sequences from the following organisms were used to generate a MUSCLE alignment: *M. jannaschii*, *M. thermoautotrophicus*, *S. acidocaldarius*, *P. denitrificans*, *S. enterica*, *S. ovata* (ArsAB), *Synechococcus* sp. WH7803, *G. kilaueensis*, *L. rosea*, *Anabaena* sp. PCC 7108, *Nostoc* sp. PCC 7524, *Synechocystis sp*. PCC 7509, *T. erythraeum*, *L. aestuarii*, *H. rivularis*, *P. minor*, *C. watsonii*, *S. meliloti* and *M. aeruginosa*. The tree was then constructed using the PhyML algorithm (100 bootstraps) with BLOSUM 62 as the model. The tree was modified for publication using the FigTree1.4.3 program available online (http://tree.bio.ed.ac.uk/software/figtree/).

RESULTS & DISCUSSION

In vivo evidence that *M. jannaschii* CobT (*Mj*CobT) is a functional enzyme.

We used an *in vivo* approach to determine whether *Mj*CobT had NaMN:DMB phoshoribosyltransferase (PRTase) activity. For this purpose, we introduced a plasmid encoding *M. jannaschii cobT*$^{+}$ into a *S. enterica* Δ*cobT* strain to try to restore AdoCbl synthesis in the absence of *Se*CobT function. ORF MJ_RS08515 (referred to as *M. jannaschii cobT*$^{+}$) was placed under the control of an arabinose-inducible promoter in plasmid pBAD24[24] to yield pMjCobT1, which was moved into strain JE12893 (Δ*cobT1379* Δ*cobB1374*) yielding strain JE18114 (Table S1).

Strain JE12893 failed to grow without exogenous Cbl (Fig. 5, triangles), but grew when Cbl was present in the medium (Fig. 5, diamonds). Ectopic expression of *M. janaschii cobT*$^{+}$ allowed strain JE18114 to grow when Cbi was present in the medium (Fig. 5, inverted triangles). This result indicated that *Mj*CobT had *Se*CobT-like activity. Strain JE18115 (Δ*cobT* Δ*cobB* / pCOBT140) served as positive control for CobT function (Fig. 5, squares).

*Mj*CobT activates diverse bases to their corresponding α-ribotides.

To gain insights into the substrate specificity of *Mj*CobT, guided biosynthesis experiments were performed. For this purpose, Cbas were extracted from *S. enterica* Δ*cobT* Δ*cobB* / p*Mj*CobT (strain JE18114) after growth in culture medium supplemented with Cbi alone or Cbi plus varying bases (*i.e.*, 5,6-dimethylbenzimidazole (DMB), adenine, 5-methoxybenzimidazole, or 5-hydroxybenzimidazole). Reverse-phase, high-performance liquid chromatography (RP-HPLC) and MALDI-TOF mass spectrometry analyses of extracted Cbas showed that all the bases tested were incorporated into the final product (Fig. 6), indicating that *Mj*CobT activated each base to its corresponding α-ribotide. Notably, when no base was provided, *Mj*CobT activated endogenous adenine and the final product was psCbl. As a positive control, the same analyses were performed with Cbas extracted from the *S. enterica* Δ*cobT* Δ*cobB* / p*Se*CobT (strain JE18115) (data not shown).

In vitro optimization of conditions for *Mj*CobT NaMN:DMB PRTase activity.

NaMN:DMB PRTase activity was measured using thin layer chromatography (TLC) and [2-^{14}C]-DMB substrate as described elsewhere[42].

Effect of pH on the reaction.—To determine optimal buffer and pH for *Mj*CobT activity, activity level was assessed using multiple buffers over a range of pH (Fig. 7). *Mj*CobT showed greatest activity at pH 10, similar to *Se*CobT[42]. Given that the internal pH of *S. enterica* is not 10, the buffer system with the highest activity within a physiologically relevant pH range was used for subsequent analyses. Subsequent experiments were performed with KP_i buffer pH 8.

***Phosphate positively affects* Mj*CobT activity*.—**Given the precedent of positive effects of phosphate on the activity of another Cba biosynthetic enzyme from a hyperthermophile[43], we varied the phosphate concentration in the reaction mixture to investigate the effect of phosphate on *Mj*CobT activity. We varied the concentration of KP_i in the reaction mixture (25–400 mM) and observed a modest increase in the amount of α-RP synthesized over a period of 15 min, from 1.0 to 1.8 nmol α-RP. To determine whether observed effect of activity was specific to phosphate, an equivalent experiment was performed with sulfate (Fig 8). The amount of DMB converted to α-RP by *Mj*CobT was measured after incubation of enzyme (250 nM) with substrates at 80°C for 15 min in the presence of sulfate, phosphate or neither. In the absence of either sulfate or phosphate the enzyme converted 0.8 nmol of DMB (40% of the initial amount) to α-RP. To assess the effect of other oxyanions on the activity of *Mj*CobT compared to phosphate, an equivalent experiment was performed with sodium salts of vanadate, selenate, or molybdate. Compared to phosphate (25 mM), none of the oxyanions tested stimulated *Mj*CobT activity, even when tested at 50 mM or 100 mM (Fig. 8).

Effect of ionic strength.—To determine the effect of salts on the activity of *Mj*CobT, varying concentrations of sodium chloride and potassium chloride were tested (100–500 mM). Altering the ionic strength of the reaction system showed no significant change in the activity of *Mj*CobT with either salt (data not shown).

***Enzyme activity as a function of temperature*.—**We also probed the effect of temperature on the activity of *Mj*CobT. As expected for an enzyme from a hyperthermophile, the activity of *Mj*CobT increased as a function of temperature, exhibiting the highest activity (~4-fold increase from 37°C) at 80°C (data not shown).

Enzyme activity as a function of NaMN.—As shown in figure 9A, the amount of *Mj*CobT-generated α-RP is displayed as a function of time for each concentration of NaMN tested. The specific activity of *Mj*CobT at each level of NaMN is shown in Figure 9B. *Mj*CobT shows NaMN:DMB PRTase activity at a physiological pH, where *Se*CobT activity was previously undetectable[42].

Effect of salting out agents.—To assess the effect of crowding agents on the activity of *Mj*CobT, varying amounts of ammonium sulfate (75–750 mM) were added to the reaction, but no significant changes in activity were observed (data not shown).

Pseudo-first order kinetics analysis of *Mj*CobT.

Kinetic parameters for the reaction catalyzed by *Mj*CobT were obtained with NaMN when DMB was provided at saturating levels (100μM). The rate of the reaction as a function of NaMN concentration is shown in figure 10 with the corresponding summary of apparent kinetic parameters shown in the inset. Kinetic parameters of *Mj*CobT for DMB were not obtained because of the limit of product detection of the assay. The plot in figure 10 is missing points below 50 μM NaMN because below that concentration product formation was not detectable. Of note, the apparent K_m of *Mj*CobT for NaMN was 5-fold lower than that of *Se*CobT[44].

Biologically active *Mj*CobT is a dimer.

The oligomeric state of *Mj*CobT was determined by analytical ultracentrifugation. *Mj*CobT protein used for this analysis was 99% homogenous (Fig. 11A). Sedimentation velocity analysis showed that 27 μM *Mj*CobT existed primarily as a 4.4 S (81.3%) species that was consistent with the expected size of a dimer (Fig. 11B). Examining the crystal structure with PISA identified a dimeric assembly with a reasonable buried interface (940 $Å^2$) and a favorable P-value of 0.164, which is good evidence of a specific, stable dimer interface[45] (Fig. 11C). The identified dimer gives a predicted sedimentation value of 4.4 S, which matches the experimentally observed species. Additional evidence supporting our identification of the dimer can be seen in the crystal structure of the distant homologue, CobT from *Pyrococcus horikoshii* (PDB 3U4G), which contains the same dimeric assembly despite a sequence identity of 37% (Fig. 11C).

The sedimentation distribution also revealed a small amount of a 6.5 S species (12.7%), which was consistent with a predicted tetramer (6.7 S) formed from the association of two of the dimers. We believe that this species is most likely caused by aggregation of the protein, with the 0.2 difference in S value being the result of the aggregate forming a less compact structure than the modeled tetramer. Finally, there was a minor peak representing 3.8% of the distribution at 0.75S. Based on the small size, this is likely a minor contaminant in the sample.

*Mj*CobT has a high affinity for NaMN substrate.

Isothermal titration calorimetry (ITC) was used to determine the affinity of *Mj*CobT for the NaMN substrate. The calculated dissociation constant (K_d) of the *Mj*CobT/NaMN complex was 3.2 μM, indicating a high affinity for the substrate (Fig. 12). Given the low concentration of NaMN in the cell[46], a high affinity for NaMN would be consistent with our expectations. ITC experiments aimed at determining the K_d of *Mj*CobT for DMB were not performed due to incompatibility of the solvent used to solubilize DMB (DMSO) with the ITC instrument. The molar ratio of ~2 was consistent with two active sites per *Mj*CobT dimer.

*Mj*CobT residues E150 and E315 are necessary for function.

In *Se*CobT, residues E174 and E317 are required for activity[47]. To investigate whether the equivalent residues in *Mj*CobT, *i.e.*, E150 and E315 (Fig. 4) were needed for activity, these residues were changed to alanine and the activity of the resulting variants was assessed *in vivo*. Concentration sweeps of DMB or adenine in the growth medium were performed to determine the minimum concentration of base necessary to confer growth of strains expressing variant proteins. Data from these experiments are shown in Table 1. In the presence of DMB (50 μM) the strain that synthesized variant *Mj*CobT^{E150A} had a doubling time similar to that of the strain that synthesized wild-type *Mj*CobT (Table 1). The strain that synthesized variant *Mj*CobT^{E150A} failed to grow when adenine (1 mM) substituted for DMB in the medium. At present it is unclear whether the *Mj*CobT^{E150A} variant could not use adenine as substrate because it cannot bind it or because it is catalytically inactive. ITC experiments aimed at answering the question of binding could not be performed due to incompatibility of the solvent needed to keep adenine in solution.

In contrast, the *Mj*CobT^{E315A} variant restored growth with 10-fold less DMB (5 μM) in the medium, suggesting that the E315A substitution did not negatively affect enzyme activity as much as the E150A substitution. Unlike *Mj*CobT^{E150A}, *Mj*CobT^{E315A} did support psCbl synthesis, even when the concentration of adenine in the medium was reduced to 0.5 mM (Table 1).

The strain that synthesized the double variant MjCobT^{E150A,E315A} failed to synthesize AdoCbl or psCbl when inoculated into medium containing DMB or adenine, suggesting that in spite of their structural differences, *Se*CobT and *Mj*CobT likely catalyze the reaction via similar mechanisms. It was previously suggested that in archaeal orthologues, an acidic residue at the position equivalent to *Se*CobT E174 might be necessary and sufficient for activity[47].

This idea was based on analyses of structural alignments which showed a valine residue in place of *Se*CobT E317 in two archaeal orthologues, one of them being *Mj*CobT. Here we show that the *Mj*CobT E315 is in fact, the equivalent to *Se*CobT E317 and both acidic residues in the active site are necessary for function *in vivo*.

*Mj*CobT homologues are commonly found in methanogenic archaea.

Using *Mj*CobT as a query sequence, we identified many homologues in both class I and class II methanogens (Table S3). Homologues identified in class I methanogens showed a high level of identity and similarity to *Mj*CobT, while class II methanogens showed a more divergent homologue. On the basis of phylogenetic analysis, *Mj*CobT is likely representative of the class of NaMN:DMB phosphoribosyltransferases found in class I methanogenic archaea.

The *cobT*$^{+}$ allele of the cyanobacterium *Synechococcus sp*. restores AdoCba biosynthesis in a CobT-deficient *S. enterica* strain when DMB is provided.

To determine whether *Synechococcus sp*. CobT had NaMN:Base PRTase activity *in vivo*, we introduced a plasmid encoding *Synechococcus sp*. WH7803 *cobT*$^{+}$ into a *S. enterica* Δ*cobT*

strain to attempt to restore AdoCbl synthesis in the absence of *Se*CobT function. ORF SYNWH7803_RS09275 (*i.e., Synecococcus cobT*$^{+}$) placed under the control of an arabinose-inducible promoter in plasmid pCV1[27] was moved into strain JE12893 (Δ*cobT* Δ*cobB*) yielding strain JE24636 (Δ*cobT* Δ*cobB* / pSynCobT2) (Table S1). Strain JE12893 failed to grow without exogenous CNCbl (Fig. 13, inverted triangles), but grew when CNCbl was present in the medium (Fig. 13, diamonds). Ectopic expression of *Synechococcus sp. cobT*$^{+}$ allowed strain JE24636 to grow when $(CN)_2$Cbi and DMB were present in the medium. Strain JE24636 failed to grow when only $(CN)_2$Cbi was provided. This result indicated *Synechococcus sp*. CobT supported *Se*CobT-like activity *in vivo* when DMB was provided (Fig. 13, triangles). Previously, cyanobacterial species were shown to solely produce psCbl. Our findings indicate *Synechococcus sp*. CobT can activate DMB, ultimately yielding AdoCbl. Strain JE18115 (Δ*cobT* Δ*cobB* / pCOBT140) served as positive control for CobT function (Fig. 13, squares).

Phylogenetic analysis suggests that CobT in cyanobacteria has an archaeal origin.

Previous studies have suggested that the majority of cyanobacterial genomes lack *cobT* and that none of the sequenced *Synechococcus* genomes encode *cobT*[17]. When searching for homologues using CobT from *S. enterica*, *P. denitrificans*, and *B. megaterium*, our findings were consistent with the data reported by Helliwell *et. al* (Table S4). With the identification of the archaeal *cobT* from *M. jannaschii*, we found numerous *cobT* homologues in the genomes of cyanobacteria, including *Synechococcus* (Table S5). The report by Helliwell *et. al*. showed that *Synechococcus* solely produced psCbl even when provided with DMB (1μM) to “guide” the biosynthesis of cobalamin. The sole synthesis of psCbl by *Synechococcus* may be attributed to a lack of DMB transport and may not indicate the exclusive production of psCbl. Our bioinformatics findings in combination with the complementation of Cbl-dependent growth by a *Synechococcus* CobT homologue suggest that cyanobacteria can activate DMB via the canonical NaMN:DMB phosphoribosyltransfer mechanism. These findings also suggest that cyanobacteria can produce Cbl in addition to psCbl.

Our phylogenetic analysis shows that the CobT homologues found in archaea and cyanobacteria cluster into a distinct clade separate from the homologues found in *Firmicutes* and proteobacteria (Fig 14). Within this clade, the majority of the cyanobacterial CobT homologues cluster tightly within a major clade and are distinctly separate from the archaeal CobTs which form another major clade. This likely suggests that the cyanobacterial CobTs are of archaeal origin and significantly differ from the CobTs found in *Firmicutes* and Proteobacteria. This difference is likely why previous studies did not identify CobT homologues in cyanobacteria.

Previous work has implicated thaumarchaeota as major Cbl producers in marine environments[16]. Previously reported genome analyses performed showed the absence of *cobT* from all thaumarchaeota and suggested that an alternative pathway for DMB activation existed in these microorganisms. Our identification of archaeal *Mj*CobT prompted the search for homologues in thaumarchaeota. We found that *cobT* is commonly found in thaumarchaeotal genomes (Table S6). Given the prevalence of *cobT* in thaumarchaeotal

genomes and the previously reported production of cobalamin, it is likely that thaumarchaeota activate DMB using a NaMN:DMB phosphoribosyltransferase enzyme.

CONCLUDING REMARKS

This study reports a new class of NaMN:DMB phosphoribosyltransferases (CobT) enzymes involved in cobamide biosynthesis in archaea and in cyanobacteria, but not in bacteria. Structurally, there are significant differences between *Mj*CobT and *Se*CobT, most notably the absence of the small domain in *Mj*CobT which is essential in forming the active site of *Se*CobT. *Mj*CobT groups with both the CobT homologues found in archaea and cyanobacteria and this group is highly divergent from the CobT homolgues found in bacteria. *Mj*CobT sequence identity compared to *Se*CobT is too low to be detected by NCBI BLASTp. Additionally, we see a greater degree of amino acid sequence similarity between *Mj*CobT and the cyanobacterial and archaeal CobT homologues than we see compared to bacterial CobT. Given this information, we feel *Mj*CobT represents a class of NaMN:DMB phosphoribosyltransferase that is significantly different from bacterial CobT. In addition, this work corrects information regarding the oligomeric state of the PRTase from *Methanocaldococcus jannaschii* (PDB 3L0Z), whose crystal structure suggests it is a trimer. Our data indicate that in solution, the biologically active *Mj*CobT enzyme is dimeric.

Supplementary Material

Refer to Web version on PubMed Central for supplementary material.

ACKNOWLEDGEMENTS

The authors have no conflict of interest to declare. This work was supported by NIH grant R37-GM040313 to J.C.E.-S.

REFERENCES

[1]. Mattes TA, Deery E, Warren MJ, and Escalante-Semerena JC (2017) Cobalamin Biosynthesis and Insertion, In Encyclopedia of Inorganic and Bioinorganic Chemistry (Scott RA, Ed.), pp 1–24, John Wiley & Sons, Ltd, Chichester, UK.

[2]. Kräutler B, Fieber W, Osterman S, Fasching M, Ongania K-H, Gruber K, Kratky C, Mikl C, Siebert A, and Diekert G (2003) The cofactor of tetrachloroethene reductive dehalogenase of Dehalospirillum multivorans is Norpseudo-B12, a new type of natural corrinoid., Helv. Chim. Acta 86, 3698–3716.

[3]. Marsh EN (1999) Coenzyme B12 (cobalamin)-dependent enzymes, Essays Biochem 34, 139–154. [PubMed: 10730193]

[4]. Yan J, Bi M, Bourdon AK, Farmer AT, Wang PH, Molenda O, Quaile AT, Jiang N, Yang Y, Yin Y, Simsir B, Campagna SR, Edwards EA, and Löffler FE (2018) Purinyl-cobamide is a native prosthetic group of reductive dehalogenases, Nat. Chem. Biol 14, 8–14. [PubMed: 29106396]

[5]. Jones AR, Rentergent J, Scrutton NS, and Hay S (2015) Probing reversible chemistry in coenzyme B12 -dependent ethanolamine ammonia lyase with kinetic isotope effects, Chemistry (Easton) 21, 8826–8831.

[6]. Bobik TA, Xu Y, Jeter RM, Otto KE, and Roth JR (1997) Propanediol utilization genes (pdu) of Salmonella typhimurium: three genes for the propanediol dehydratase., J. Bacteriol 179, 6633–6639. [PubMed: 9352910]

[7]. Sofia HJ, Chen G, Hetzler BG, Reyes-Spindola JF, and Miller NE (2001) Radical SAM, a novel protein superfamily linking unresolved steps in familiar biosynthetic pathways with radical

mechanisms: functional characterization using new analysis and information visualization methods., Nucleic Acids Res 29, 1097–1106. [PubMed: 11222759]

[8]. Padmanabhan S, Jost M, Drennan CL, and Elias-Arnanz M (2017) A new facet of vitamin B12: Gene regulation by cobalamin-based photoreceptors, Annu. Rev. Biochem 86, 485–514. [PubMed: 28654327]

[9]. Renz P (1999) Biosynthesis of the 5,6-dimethylbenzimidazole moiety of cobalamin and of other bases found in natural corrinoids, In Chemistry and Biochemistry of B12 (Banerjee R, Ed.), pp 557–575, John Wiley & Sons, Inc., New York.

[10]. Johnson MG, and Escalante-Semerena JC (1992) Identification of 5,6-dimethylbenzimidazole as the Coα ligand of the cobamide synthesized by Salmonella typhimurium. Nutritional characterization of mutants defective in biosynthesis of the imidazole ring, J. Biol. Chem 267, 13302–13305. [PubMed: 1618831]

[11]. Keck B, and Renz P (2000) Salmonella typhimurium forms adenylcobamide and 2-methyladenylcobamide, but no detectable cobalamin during strictly anaerobic growth, Arch. Microbiol 173, 76–77. [PubMed: 10648108]

[12]. Anderson PJ, Lango J, Carkeet C, Britten A, Kräutler B, Hammock BD, and Roth JR (2008) One pathway can incorporate either adenine or dimethylbenzimidazole as an alpha-axial ligand of B_{12} cofactors in Salmonella enterica, J. Bacteriol 190, 1160–1171. [PubMed: 17981976]

[13]. Trzebiatowski JR, and Escalante-Semerena JC (1997) Purification and characterization of CobT, the nicotinate-mononucleotide:5,6-dimethylbenzimidazole phosphoribosyltransferase enzyme from Salmonella typhimurium LT2, J. Biol. Chem 272, 17662–17667. [PubMed: 9211916]

[14]. Cheong CG, Escalante-Semerena JC, and Rayment I (2001) Structural investigation of the biosynthesis of alternative lower ligands for cobamides by nicotinate mononucleotide: 5,6-dimethylbenzimidazole phosphoribosyltransferase from Salmonella enterica, J. Biol. Chem 276, 37612–37620. [PubMed: 11441022]

[15]. Hazra AB, Tran JL, Crofts TS, and Taga ME (2013) Analysis of substrate specificity in CobT homologs reveals widespread preference for DMB, the lower axial ligand of vitamin B(12), Chem. Biol 20, 1275–1285. [PubMed: 24055005]

[16]. Heal KR, Qin W, Ribalet F, Bertagnolli AD, Coyote-Maestas W, Hmelo LR, Moffett JW, Devol AH, Armbrust EV, Stahl DA, and Ingalls AE (2017) Two distinct pools of B12 analogs reveal community interdependencies in the ocean, Proc. Natl. Acad. Sci. U S A 114, 364–369. [PubMed: 28028206]

[17]. Helliwell KE, Lawrence AD, Holzer A, Kudahl UJ, Sasso S, Krautler B, Scanlan DJ, Warren MJ, and Smith AG (2016) Cyanobacteria and eukaryotic algae use different chemical variants of vitamin B12, Curr. Biol 26, 999–1008. [PubMed: 27040778]

[18]. Berkowitz D, Hushon JM, Whitfield HJ, Jr., Roth J, and Ames BN (1968) Procedure for identifying nonsense mutations, J. Bacteriol 96, 215–220. [PubMed: 4874308]

[19]. Balch WE, Fox GE, Magrum LJ, Woese CR, and Wolfe RS (1979) Methanogens: reevaluation of a unique biological group, Microbiol. Rev 43, 260–296. [PubMed: 390357]

[20]. O'Toole GA, Rondon MR, and Escalante-Semerena JC (1993) Analysis of mutants of defective in the synthesis of the nucleotide loop of cobalamin, J. Bacteriol 175, 3317–3326. [PubMed: 8501035]

[21]. Maniatis T, Fritsch EF, and Sambrook J (1982) Introduction of plasmid and bacteriophage lambda into Escherichia coli, In Molecular cloning: a laboratory manual (Maniatis T, Fritsch EF, and Sambrook J, Eds.), pp 250–251, Cold Spring Harbor Laboratory, Cold Spring Harbor, New York.

[22]. Datsenko KA, and Wanner BL (2000) One-step inactivation of chromosomal genes in Escherichia coli K-12 using PCR products., Proc. Natl. Acad. Sci. USA 97, 6640–6645. [PubMed: 10829079]

[23]. Klock HE, Koesema EJ, Knuth MW, and Lesley SA (2008) Combining the polymerase incomplete primer extension method for cloning and mutagenesis with microscreening to accelerate structural genomics efforts, Prot.-Struct. Funct. Bioinformat 71, 982–994.

[24]. Guzman LM, Belin D, Carson MJ, and Beckwith J (1995) Tight regulation, modulation, and high-level expression by vectors containing the arabinose PBAD promoter, J. Bacteriol 177, 4121–4130. [PubMed: 7608087]

[25]. Rocco CJ, Dennison KL, Klenchin VA, Rayment I, and Escalante-Semerena JC (2008) Construction and use of new cloning vectors for the rapid isolation of recombinant proteins from Escherichia coli, Plasmid 59, 231–237. [PubMed: 18295882]

[26]. Mattes TA, and Escalante-Semerena JC (2017) Salmonella enterica synthesizes 5,6-dimethylbenzimidazolyl-(DMB)-alpha-riboside. Why some Firmicutes do not require the canonical DMB activation system to synthesize adenosylcobalamin, Mol. Microbiol 103, 269–281.

[27]. VanDrisse CM, and Escalante-Semerena JC (2016) New high-cloning-efficiency vectors for complementation studies and recombinant protein overproduction in Escherichia coli and Salmonella enterica, Plasmid 86, 1–6. [PubMed: 27234933]

[28]. Kittaka-Katsura H, Fujita T, Watanabe F, and Nakano Y (2002) Purification and characterization of a corrinoid compound from Chlorella tablets as an algal health food, J. Agric. Food Chem 50, 4994–4997. [PubMed: 12166996]

[29]. Keller S, Treder A, SH VR, Escalante-Semerena JC, and Schubert T (2016) The SMUL_1544 gene product governs norcobamide biosynthesis in the tetrachloroetheneres piring bacterium Sulfurospirillum multivorans, J. Bacteriol 198, 2236–2243. [PubMed: 27274028]

[30]. Blanche F, Thibaut D, Couder M, and Muller JC (1990) Identification and quantitation of corrinoid precursors of cobalamin from Pseudomonas denitrificans by high-performance liquid chromatography, Anal. Biochem 189, 24–29. [PubMed: 2278386]

[31]. Chan CH, and Escalante-Semerena JC (2011) ArsAB, a novel enzyme from Sporomusa ovata activates phenolic bases for adenosylcobamide biosynthesis, Mol. Microbiol 81, 952–967. [PubMed: 21696461]

[32]. Sambrook J, Fritsch EF, and Maniatis T (1989) Molecular Cloning: A Laboratory Manual, Second ed, Cold Spring Harbor Laboratory, Cold Spring Harbor, N.Y.

[33]. Blommel PG, and Fox BG (2007) A combined approach to improving large-scale production of tobacco etch virus protease, Protein Expr. Purif 55, 53–68. [PubMed: 17543538]

[34]. Gasteiger E, Gattiker A, Hoogland C, Ivanyi I, Appel RD, and Bairoch A (2003) ExPASy: The proteomics server for in-depth protein knowledge and analysis, Nucleic Acids Res 31, 3784–3788. [PubMed: 12824418]

[35]. Laue TM, Shah BD, and Ridgeway TM (1992) Analytical ultracentrifugation in biochemistry and polymer science, R. Soc. Chem, 90–125.

[36]. Laue TM, Shah BD, Ridgeway TM, and Pelletier SL (1992) Analytical Ultracentrifugation in Biochemistry and Polymer Science, R. Soc. Chem, 90–125.

[37]. Schuck P (2003) On the analysis of protein self-association by sedimentation velocity analytical ultracentrifugation, Anal. Biochem 320, 104–124. [PubMed: 12895474]

[38]. Ortega A, Amoros D, and Garcia de la Torre J (2011) Prediction of hydrodynamic and other solution properties of rigid proteins from atomic- and residue-level models, Biophys. J 101, 892–898. [PubMed: 21843480]

[39]. Altschul SF, Madden TL, Schaffer AA, Zhang J, Zhang Z, Miller W, and Lipman DJ (1997) Gapped BLAST and PSI-BLAST: a new generation of protein database search programs, Nucleic Acids Res 25, 3389–3402. [PubMed: 9254694]

[40]. Marchler-Bauer A, Anderson JB, Chitsaz F, Derbyshire MK, DeWeese-Scott C, Fong JH, Geer LY, Geer RC, Gonzales NR, Gwadz M, He S, Hurwitz DI, Jackson JD, Ke Z, Lanczycki CJ, Liebert CA, Liu C, Lu F, Lu S, Marchler GH, Mullokandov M, Song JS, Tasneem A, Thanki N, Yamashita RA, Zhang D, Zhang N, and Bryant SH (2009) CDD: specific functional annotation with the Conserved Domain Database, Nucleic Acids Res 37, D205–210. [PubMed: 18984618]

[41]. Gouy M, Guindon S, and Gascuel O (2010) SeaView version 4: A multiplatform graphical user interface for sequence alignment and phylogenetic tree building, Mol. Biol. Evol 27, 221–224. [PubMed: 19854763]

[42]. Claas KR, Parrish JR, Maggio-Hall LA, and Escalante-Semerena JC (2010) Functional analysis of the nicotinate mononucleotide:5,6-dimethylbenzimidazole phosphoribosyltransferase (CobT)

enzyme, involved in the late steps of coenzyme B12 biosynthesis in Salmonella enterica, J. Bacteriol 192, 145–154. [PubMed: 19880598]

[43]. Woodson JD, and Escalante-Semerena JC (2006) The cbiS gene of the archaeon Methanopyrus kandleri AV19 encodes a bifunctional enzyme with adenosylcobinamide amidohydrolase and alpha-ribazole-phosphate phosphatase activities, J. Bacteriol 188, 4227–4235. [PubMed: 16740929]

[44]. Maggio-Hall LA, and Escalante-Semerena JC (2003) Alpha-5,6-Dimethylbenzimidazole adenine dinucleotide (alpha-DAD), a putative new intermediate of coenzyme B12 biosynthesis in Salmonella typhimurium, Microbiology 149, 983–990. [PubMed: 12686640]

[45]. Krissinel E, and Henrick K (2007) Inference of macromolecular assemblies from crystalline state, J. Mol. Biol 372, 774–797. [PubMed: 17681537]

[46]. Bochner BR, and Ames BN (1982) Complete analysis of cellular nucleotides by two-dimensional thin layer chromatography, J. Biol. Chem 257, 9759–9769. [PubMed: 6286632]

[47]. Chan CH, Newmister SA, Talyor K, Claas KR, Rayment I, and Escalante-Semerena JC (2014) Dissecting cobamide diversity through structural and functional analyses of the base-activating CobT enzyme of Salmonella enterica, Biochim. Biophys. Acta 1840, 464–475. [PubMed: 24121107]

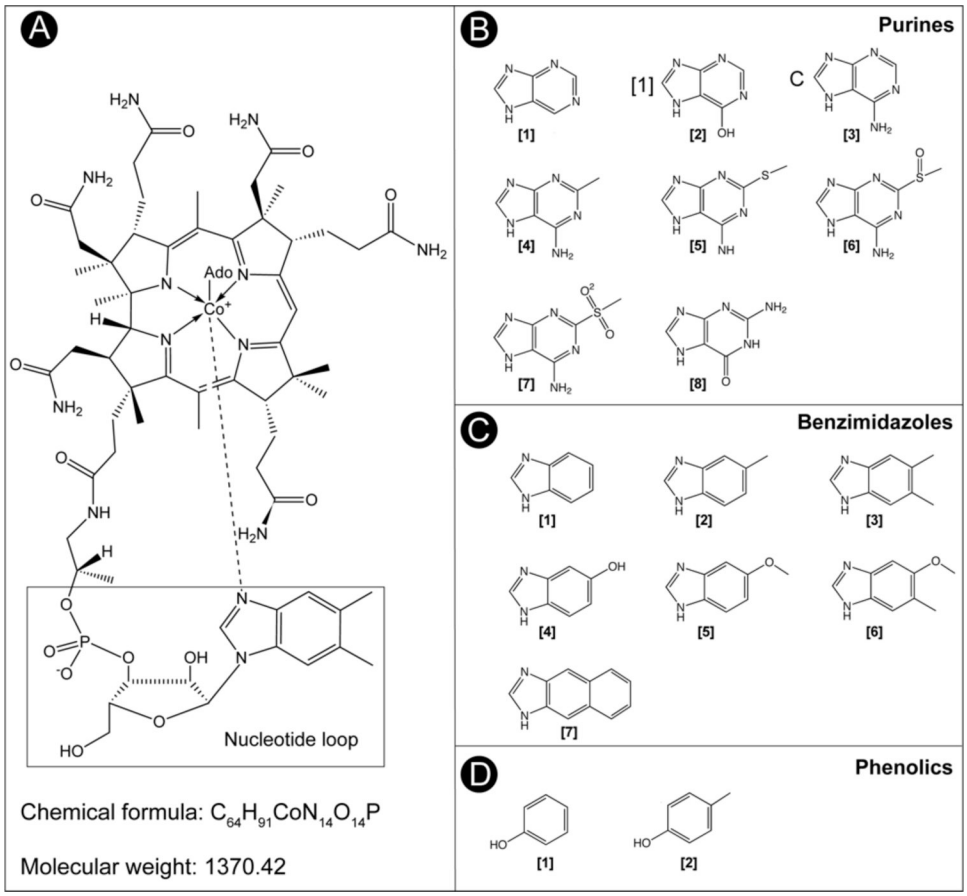

Figure 1. Adenosylcobamide (AdoCba) structure and nucleotide base diversity.

A. The nucleotide loop is boxed. B. Purines and purine analogues found in Cbas: [1], purine; [2]. hypoxanthine; [3], adenine; [4], 2-methyladenine; [5], 2-methylmercaptoadenine; [6], 2-methylsulfinyladenine; [7], 2-methylsulfonyladenine; [8], guanine. C. Benzimidazole and its analogues: [1], benzimidazole; [2], 5-methylbenzimidazole; [3], 5,6-dimethylbenzimidazole; [4], 5-hydroxybenzimidazole; [5], 5-methoxybenzimidazole; [6], 5-methoxy-6-methylbenzimidazole; [7], naphthimidazole. D. Phenolics: [1], phenol; [2], *p*-cresol.

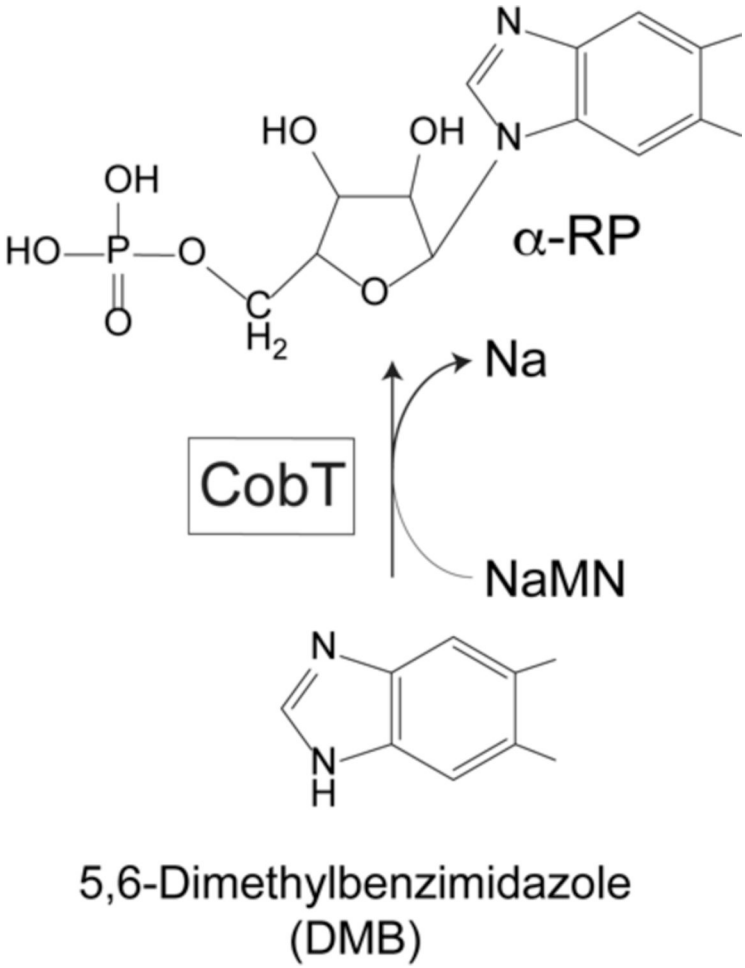

Figure 2. Base Activation by CobT.

The activation of 5,6-dimethylbenzimidazole (DMB) to its α-ribotide by CobT PRTase is shown. NaMN, nicotinate mononucleotide, Na, nicotinic acid, α-RP, alpha-ribazole-phosphate, CobT: NaMN:DMB phosboribosyltransferase (EC 2.4.2.21)

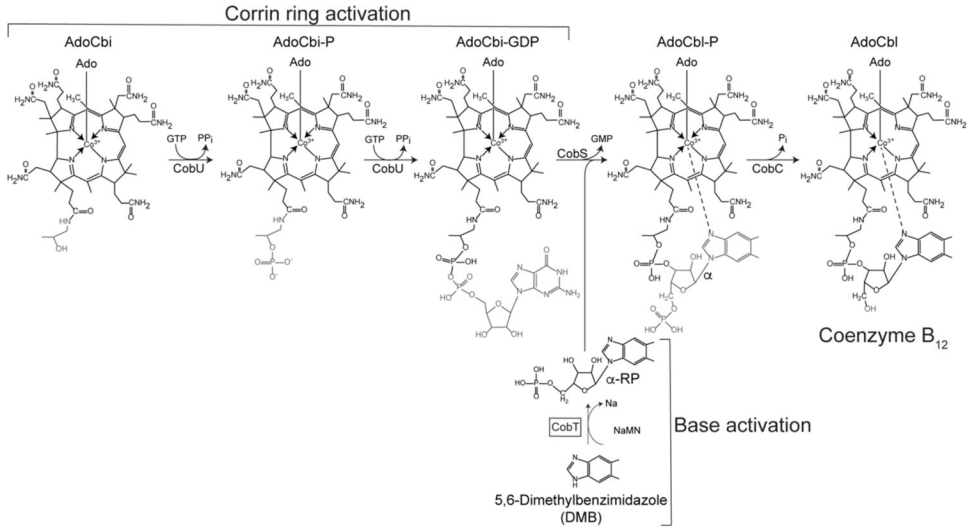

Figure 3. Late steps of coenzyme B_{12} biosynthesis.

This figure schematizes the two branches of the nucleotide loop assembly (NLA) pathway that yields coenzyme B_{12} in *S. enterica*. This bacterium can assimilate exogenous, incomplete corrinoids such as cobinamide (Cbi) converting it to AdoCbi and activating it to AdoCbi-GDP via AdoCbi-P using the bifunctional kinase/guanylyltransferase (CobU) enzyme. The base shown in this scheme is 5,6-dimethylbenzimidazole (DMB), which is activated to its α-ribotide by the CobT PRTase (shown inside the box). Condensation of the activated intermediates followed by dephosphorylation yields biologically active coenzyme B_{12}.

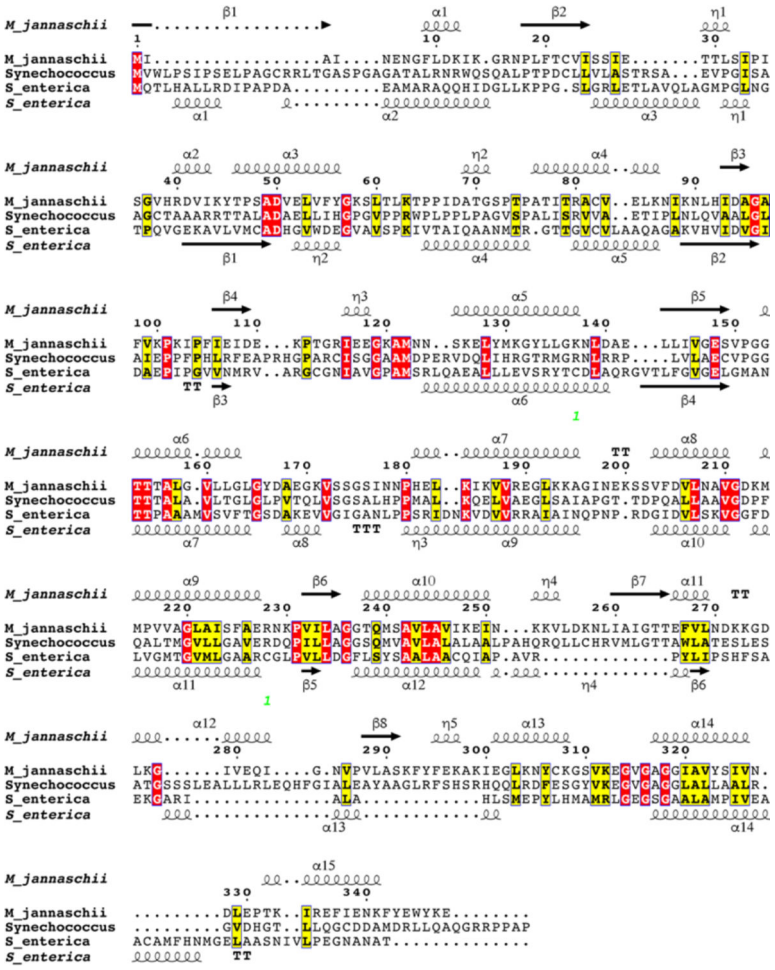

Figure 4. Protein sequence similarities and identities among *Mj*CobT, *Se*CobT, and *Synechococcus* CobT.

The alignment was generated using Clustal Omega and visualized with ESPript 3.0 web-based program. Alpha helices and beta sheets for *Mj*CobT (PDB 3L0Z) and *Se*CobT (PDB 1L4B) obtained from the reported crystal apo structures are shown. The structure of *Synechococcus* CobT has not been reported.

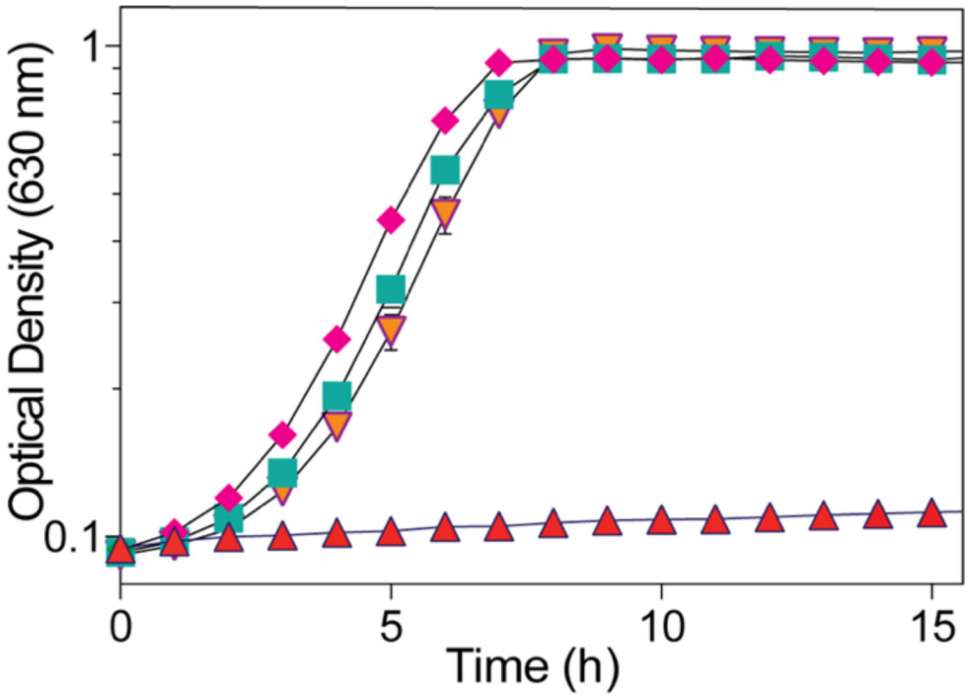

Figure 5. *Mj*CobT supports AdoCbl-dependent growth of *S. enterica*.

Strains were grown in minimal NCE medium supplemented with ribose (20 mM) as carbon and energy source. $(CN)_2$Cbi (15 nM) was added to all cultures, except to the culture growing in the presence of CNCbl (diamonds). DMB (150 μM) was added to all cultures except for the culture to which CNCbl was added (diamonds).

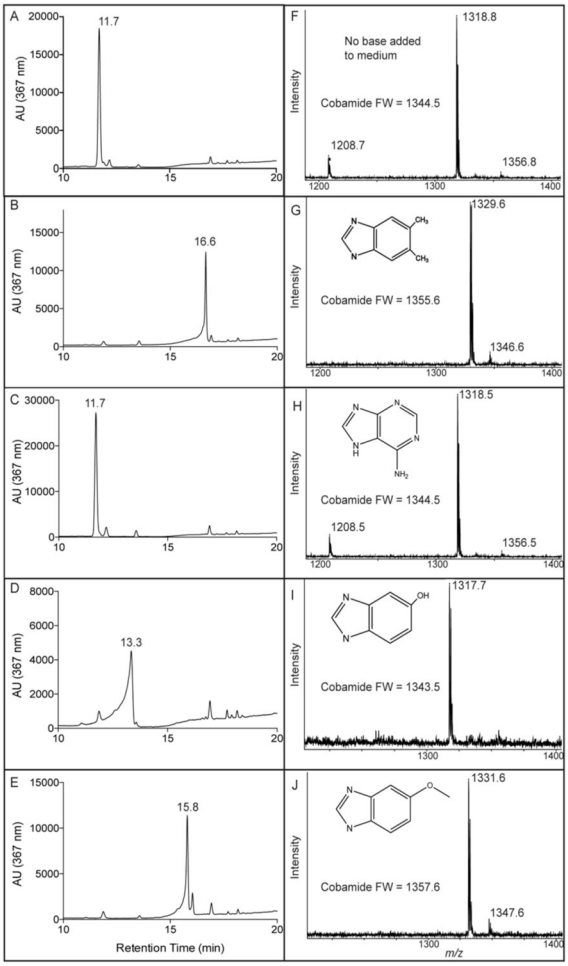

Figure 6. *Mj*CobT can activate different bases.

The figure shows RP-HPLC tracings (panels A-E) and MALDI-TOF mass spectra (panels F-J) of α-ribotides synthesized by *Mj*CobT under conditions described under *Materials and Methods*. The substrates used were: 5,6-dimethylbenzymidazole (panels B, G), adenine (panels C, H), 5-hydroxybenzimidazole (panels D, I), and 5-methoxybenzimidazole (panels (E, J).

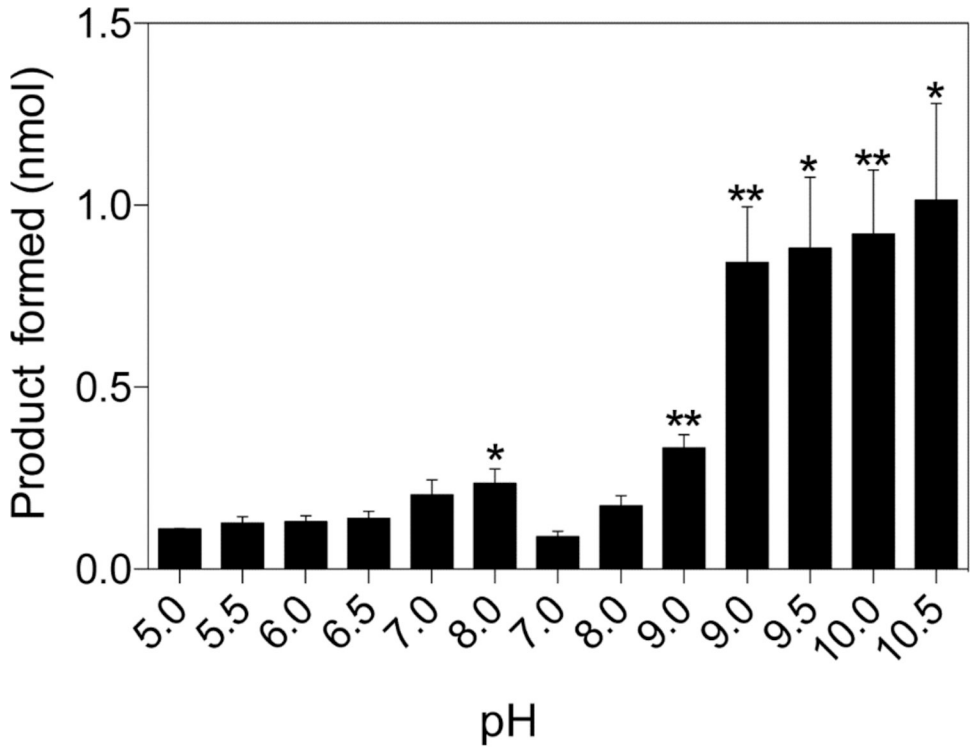

Figure 7. Effect of pH on *Mj*CobT activity.

Conditions for the PRTase reaction are described under *Materials and Methods*. Product formation is displayed as a function of pH. Error bars represent the standard error of the mean. Asterisks represent significance determined by unpaired T test compared to pH 7. The following buffers were tested in order of appearance: sodium malate (pH 5), sodium succinate (pH 5.5), MES (pH 6), 2-[Bis(2-hydroxyethyl)amino]-2-(hydroxymethyl)propane-1,3-diol (Bis-Tris, pH 6.5), imidazole (pH 7), phosphate (pH 8), 2-amino-2-(hydroxymethyl)-1,3-propanediol chloride (Tris-HCl pH 7, 8, 9), *N*-cyclohexyl-2-aminoethanesulfonic acid (CHES pH 9, 9.5), and glycine (pH 10, 10.5).

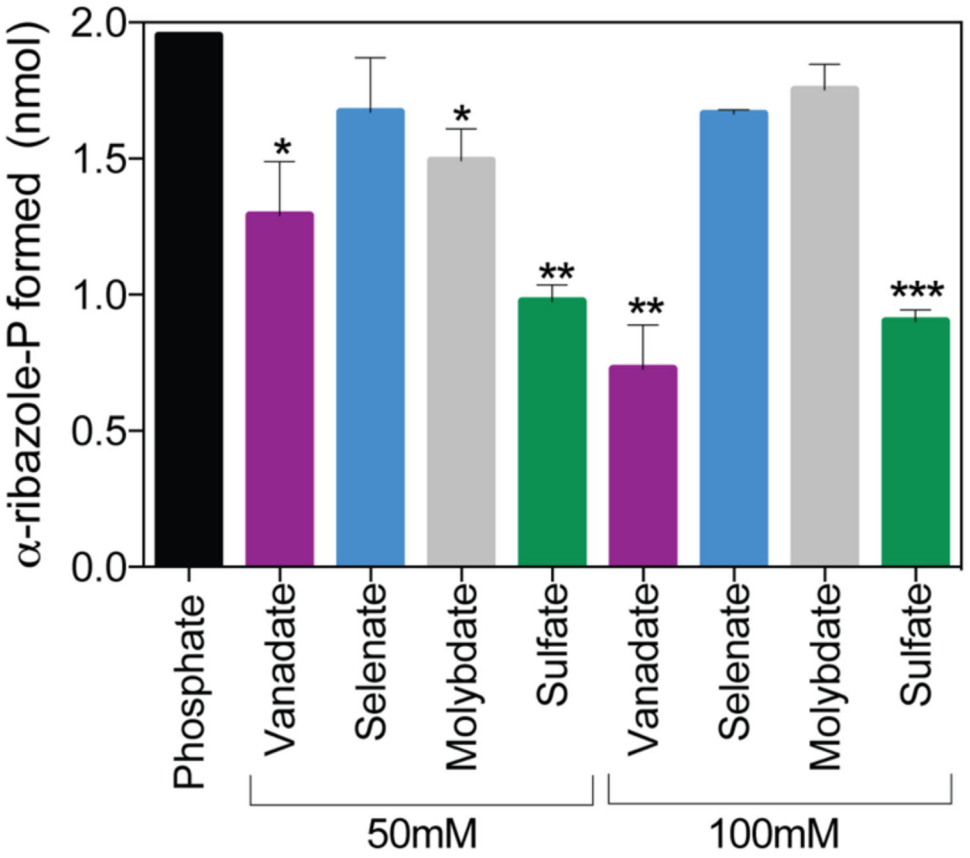

Figure 8. Phosphate positively affects *Mj*CobT activity, vanadate, selenate, molybdate and sulfate do not.

Conditions for the PRTase reaction are described under *Materials and Methods*. Product formation is shown for each oxyanion provided at 50 mM and 100 mM compared to 25 mM phosphate. Error bars represent the standard error of the mean. Asterisks show significance determined by unpaired T test compared to phosphate condition.

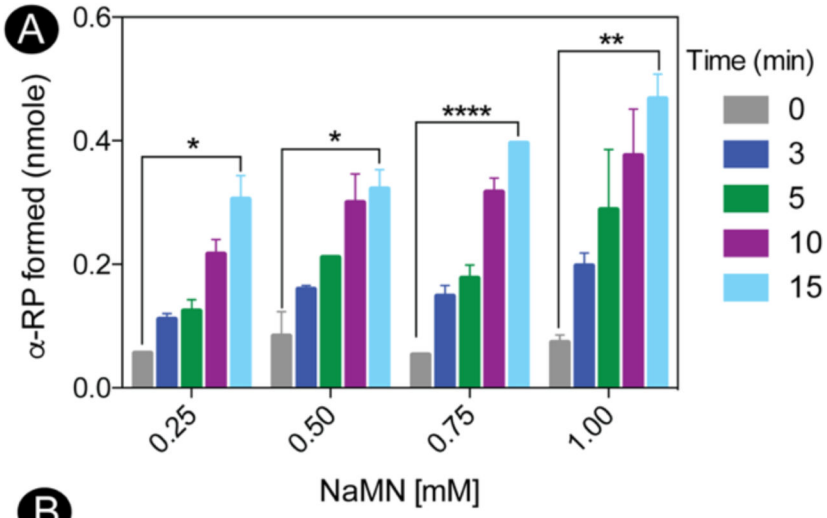

B

NaMN [mM]	Specific Activity (nmol/min/mg)
0.25	87 ± 18
0.5	95 ± 9
0.75	121 ± 7
1	132 ± 11

Figure 9. *Mj*CobT activates 5,6- dimethylbenzimidazole to α-ribazole- phosphate (α-RP). Conditions for the PRTase reaction are described under *Materials and Methods*. In panel A, product formation is shown as a function of time across varying NaMN concentrations. Product formation was quantified as a function of time. Error bars represent standard error of the mean. Asterisks shown significance determined by unpaired T test comparing time 0 to time 15. Panel B shows average specific activities with standard deviations for each concentration of NaMN tested.

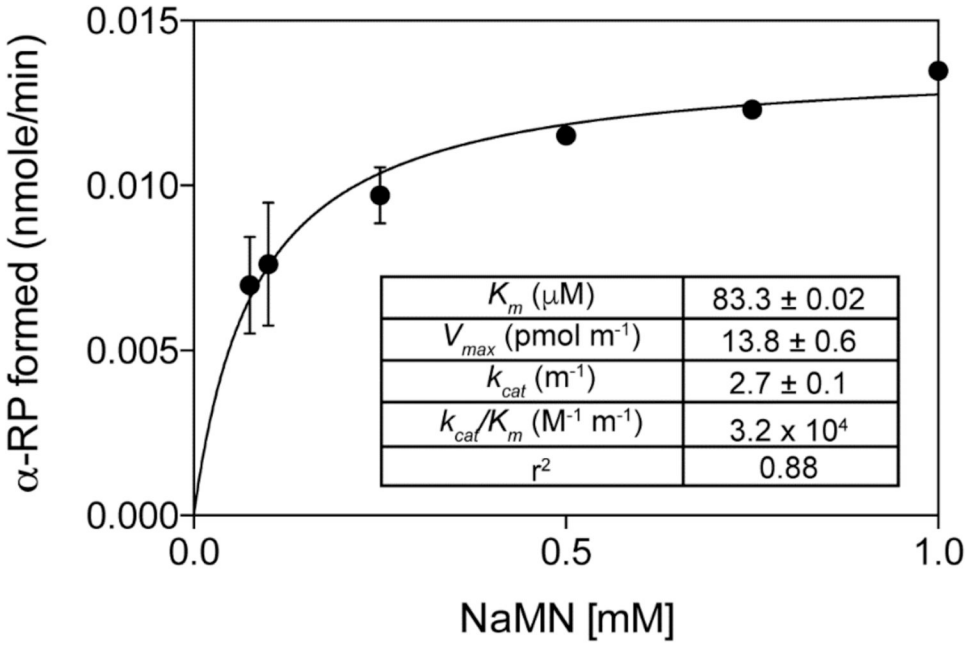

Figure 10. Pseudo-first order kinetics of the *Mj*CobT reaction as a function of NaMN.

In all reaction mixtures DMB was present at saturating levels (100 μM). Details of the protocol used can be found under *Materials and Methods*. Apparent kinetic parameters are shown in the inset.

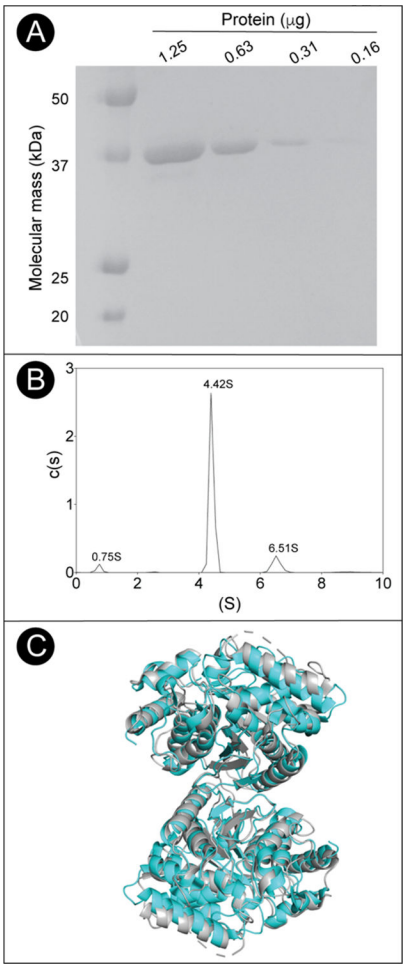

Figure 11. Oligomeric state and purity of MyOobT.

A. SDS-PAGE behavior of *Mj*CobT compared to BioRad Precision Plus Protein Standards. Based on the data shown in panel B, *Mj*CobT was estimated to be >99% homogeneous. B. Sedimentation velocity c(s) distribution of *Mj*CobT at pH7.5 showing three species at 0.75 S, 4.42 S, and 6.51 S C. Cartoon model of the *Mj*CobT dimer (cyan) identified in the crystal structure (PDB ID 3L0Z) superimposed onto the homologous CobT from *Pyrococcus horikoshii* dimer in grey (PDB ID 3U4G).

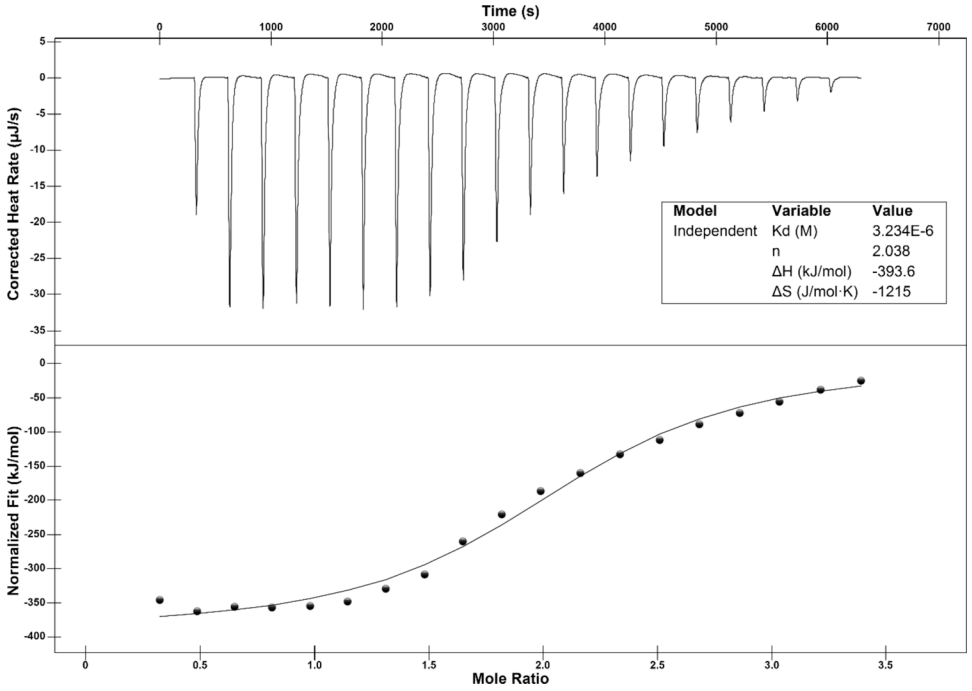

Figure 12. ITC analysis of NaMN binding to *Mj*CobT.

Sample preparation for ITC analysis is described in detailed under *Materials and Methods*. Twenty 2.4-µL injections of 1 mM NaMN spaced every 5 min were made during the course of the experiment. The top panel shows the heat released per injection. The interaction between *Mj*CobT and NaMN is shown as enthalpy per mol of NaMN injected as a function of the molar ratio of protein to ligand (bottom panel). The binding isotherm was obtained from the integrals of the peaks. Shown in the inset are the best-fit values for the dissociation constant (K_d), stoichiometry (n), enthalpic change (ΔH), and entropic change (ΔS).

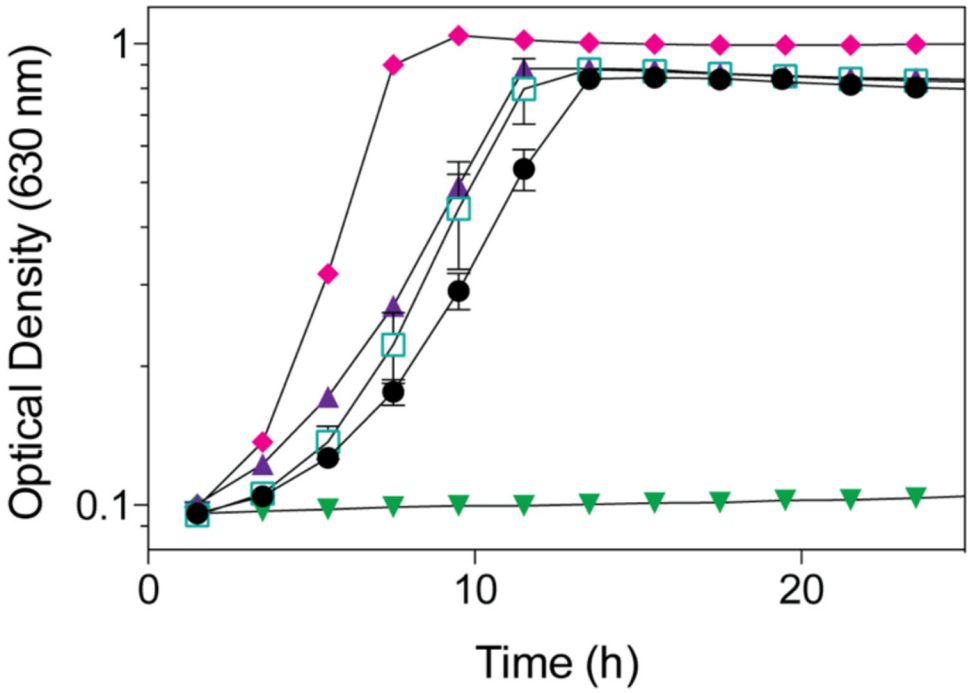

Figure 13. *Synechococcus* CobT supports AdoCbl-dependent growth of *S. enterica* in the absence of *cobT* and *cobB*.

S. enterica strains were grown in minimal medium supplemented with ribose (20 mM). $(CN)_2$Cbi (15 nM) and DMB (150 μM) were added to all cultures except to the one to which CNCbl was added (diamonds). *Synechococcus* CobT (triangles) and *Se*CobT (squares) were expressed *in trans* in a Δ*cobT* Δ*cobB S. enterica* strain. A *cobT*$^+$ *cobB*$^+$ *S. enterica* strain (circles) served as positive control. A *S. enterica* strain deficient in CobT and CobB activity served as negative control (inverted triangles).

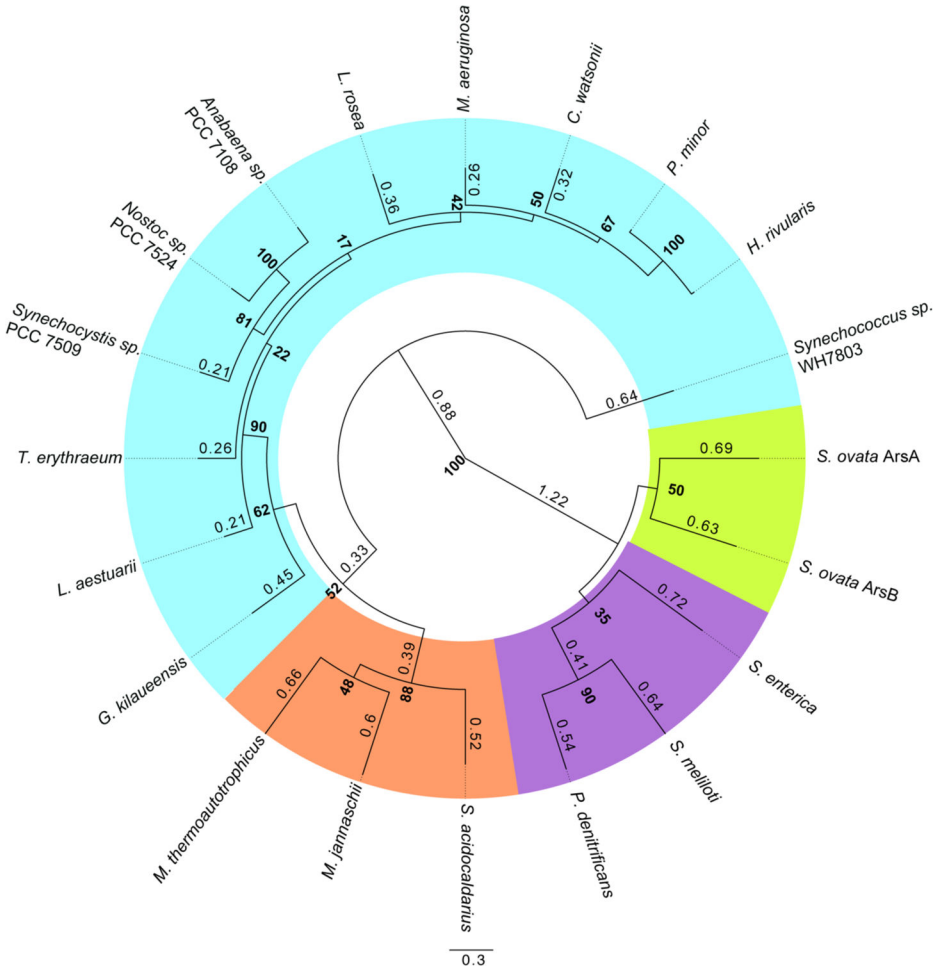

Figure 14. Cyanobacterial CobT homologues are of archaeal origin.

Phylogenetic relationship of CobT homologues from diverse archaea and bacteria are shown. The tree was built based on a MUSCLE alignment using PhyML algorithm with BLOSUM62 model (100 bootstraps). Bootstrap values are presented in bold at the nodes and branch times are shown to 2 significant figures. Branch times below 0.2 were omitted from the tree. Organism highlighting is as follows: cyanobacteria in blue, archaea in orange, proteobacteria in purple, and *Firmicutes* in green.

Table 1.

Doubling times (h) of a *S. enterica cobT cobB* strain harboring plasmids encoding *Mj*CobT proteins

Variant (plasmid)	Cbi (15 nM)	Cbi + DMB	Cbi + Ade	Cbl (100 nM)
Vector (pBAD24)	NG	NG	NG	1.2 ± 0.01[3 h lag]
***Mj*CobT^{WT} (pMjCobT1)**	1.6 ± 0.01 [3 h lag]	1.4 ± 0.01, [3 h lag] (10 nM)	1.5 ± 0.01, [3 h lag] (10 nM)	1.2 ± 0.01, [3 h lag]
***Mj*CobT^{E150A} (pMjCobT5)**	NG	2.0 ± 0.02, [3 h lag] (50 μM) 3.4 ± 0.12, [20 h lag] (1 μM)	NG (1mM)	1.5 ± 0.01, [4 h lag]
***Mj*CobT^{E315A} (pMjCobT3)**	NG	1.6 ± 0.01, [3 h lag] (5 μM) 2.0 ± 0.19[19 h lag] (50 nM)	2.2 ± 0.03, [6 h lag] (0.5 mM)	1.8 ± 0.03, [4 h lag]
MjCobT$^{E150A\ E315A}$ (pMjCobT4)	NG	NG	NG	1.9 ± 0.17, [4 h lag]

Cells were grown in NCE minimal medium supplemented with ribose (20mM) as the sole carbon and energy source. Doubling times are shown in hours with the standard error of the mean. Lag times are shown in brackets. Concentrations of added ring precursor or base are shown in parenthesis. NG, no growth; Cbi, dicyanocobinamide [$(CN)_2$Cbi]; DMB, 5,6-dimethylbenzimidazole; Cbl, cyanocobalamin (CNCbl, vitamin B_{12}); Ade, adenine